ORGANIC LETTERS

2013
Vol. 15, No. 20
5322–5325

Synthesis of *P*-Triazole Dithienophospholes and a Cyclodextrin-Based Sensor via Click Chemistry

Xiaoming He, Ping Zhang, Jian-Bin Lin, Huy V. Huynh, Sandra E. Navarro Muñoz, Chang-Chun Ling, and Thomas Baumgartner*

Department of Chemistry and Centre for Advanced Solar Materials, University of Calgary, 2500 University Drive NW, Calgary, AB T2N 1N4, Canada

thomas.baumgartner@ucalgary.ca

Received September 6, 2013

ABSTRACT

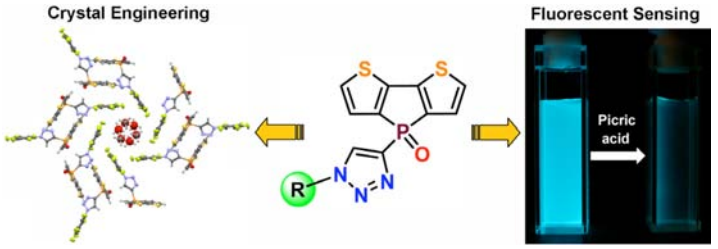

The synthesis of a series of highly luminescent, functional dithienophospholes via a click reaction is reported. Slight modification of the lateral aromatic substituents leads to a significant difference in their solid-state organization. In addition, a novel water-soluble β-cyclodextrin hybrid is demonstrated to be an effective sensor for picric acid.

By virtue of their unique bonding and electronic properties, the incorporation of main-group elements (e.g., B, Si, P) offers great opportunities for efficiently tuning the optoelectronic properties of π-conjugated materials at the molecular level.[1−3] Phosphole-based π-conjugated compounds, in particular, have attracted significant attention because of the versatile reactivity of the P center that endows these materials with tunable photophysical and redox properties, as well as interesting molecular organization and self-assembly.[3] Systematic studies by others and our group have revealed that the LUMO energies of the phosphole derivatives are stabilized through $\sigma^*-\pi^*$ orbital coupling, which also makes phosphole-based materials very promising electron-acceptor materials.[3]

Over the past decade, we have established the dithieno-[3,2-*b*:2′,3′-*d*]phosphole (Figure 1) as a unique building block for the development of highly emissive materials.[4] To date, most efforts have invested on the *P*-phenyl species (**I**) for tuning the optoelectronic and self-assembly properties of the system via introduction of different aromatic groups on the conjugated backbone (at R^1 and R^2), or simple modification of the phosphorus center (E = lone pair, O, S, Me^+, BH_3, and metals).[4e] In doing so, we were able to successfully utilize this intriguing building block in a variety of different functional materials such as white-light emitting species,[5] sensors,[6] liquid crystals, and

(1) (a) Jäkle, F. *Chem. Rev.* **2010**, *110*, 3985–4022. (b) Wade, C. R.; Broomsgrove, A. E. J.; Aldrige, S.; Gabbaï, F. P. *Chem. Rev.* **2010**, *110*, 3958–3984. (c) Hudson, Z. M.; Wang, S. *Acc. Chem. Res.* **2009**, *42*, 1584–1596.

(2) (a) Yamaguchi, S.; Tamao, K. *J. Chem. Soc., Dalton Trans.* **1998**, 3693–3702. (b) Chen, J.; Cao, Y. *Macromol. Rapid Commun.* **2007**, *28*, 1714–1742.

(3) (a) Baumgartner, T.; Réau, R. *Chem. Rev.* **2006**, *106*, 4681–4727. Correction: **2007**, *107*, 303. (b) Crassous, J.; Réau, R. *Dalton Trans.* **2008**, 6865–6876. (c) Matano, Y.; Imahori, H. *Org. Biomol. Chem.* **2009**, *7*, 1258–1271. (d) Ren, Y.; Baumgartner, T. *Dalton Trans.* **2012**, *41*, 7792–7800. (e) Fukazawa, A.; Yamaguchi, S. *Chem. Asian J.* **2009**, *4*, 1386–1400.

(4) (a) Baumgartner, T.; Neumann, T.; Wirges, B. *Angew. Chem., Int. Ed.* **2004**, *43*, 6197–6201. (b) Baumgartner, T.; Bergmans, W.; Kárpáti, T.; Neumann, T.; Nieger, M.; Nyulászi, L. *Chem.—Eur. J.* **2005**, *11*, 4687–4699. (c) Dienes, Y.; Durben, S.; Kárpáti, T.; Neumann, T.; Englert, U.; Nyulászi, L.; Baumgartner, T. *Chem.—Eur. J.* **2007**, *13*, 7487–7500. (e) Romero-Nieto, C.; Baumgartner, T. *Synlett* **2013**, *24*, 920–937.

(5) (a) Romero-Nieto, C.; Durben, S.; Kormos, I. M.; Baumgartner, T. *Adv. Funct. Mater.* **2009**, *19*, 3625–3631. (b) Huynh, H. V.; He, X. M.; Baumgartner, T. *Chem. Commun.* **2013**, *49*, 4899–4901.

(6) Neumann, T.; Dienes, Y.; Baumgartner, T. *Org. Lett.* **2006**, *8*, 495–497.

(7) (a) Ren, Y.; Kan, W. H.; Henderson, M. A.; Bomben, P. G.; Berlinguette, C. P.; Thangadurai, V.; Baumgartner, T. *J. Am. Chem. Soc.* **2011**, *133*, 17014–17026. (b) Ren, Y.; Kan, W. H.; Thangadurai, V.; Baumgartner, T. *Angew. Chem., Int. Ed.* **2012**, *51*, 3964–3968.

10.1021/ol402582p
Published on Web 09/30/2013

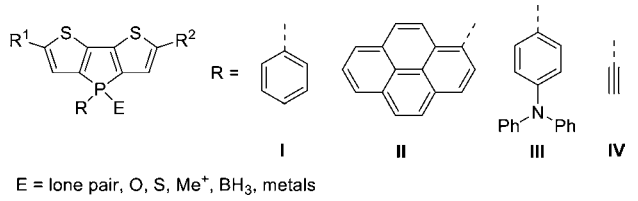

Figure 1. Structures of dithieno[3,2-*b*:2′,3′-*d*]phospholes.

organogels.[7] In addition, we have revealed that replacement of the *P*-phenyl group with other polyaromatic hydrocarbon substituents (e.g., **II**) or the electron-donating triphenylamine (**III**) leads to charge- and electron-transfer properties, as well as interesting molecular packing.[8] Very recently, we have reported a novel class of phospholes with an alkynyl group at the P center (**IV**), by which the self-assembly behavior can easily be tuned using the highly efficient "click" reaction. This synthetic strategy affords a *P*-triazole substituent, which was proposed to simply behave as a linker, akin to its *P*-phenyl congener.[9]

Herein, we further elucidate the molecular structures of *P*-triazole dithienophospholes and the role the triazole plays for their solid-state organization. In this context, the tunability of the photophysical properties via lateral substituents (**1**–**3**) was also investigated (Scheme 1). In addition, we report a novel water-soluble dithienophosphole **4** by hybridization with a β-cyclodextrin (β-CD) that is a well-known supramolecular host to bind a variety of organic molecules,[10] as well as its application as fluorescent sensor for picric acid in aqueous media.

Compounds **1**–**4** were synthesized in high yield (80–90%) via a Huisgen click reaction from the precursor dithienophosphole (**A**) with corresponding azides, according to our previously reported procedure.[9] Details on the synthesis are given in the Supporting Information. All new compounds were fully characterized by ^{1}H, ^{13}C, and ^{31}P NMR spectroscopy, as well as high-resolution mass spectrometry. Transforming the alkynyl moiety (δ^{31}P **A**: −10.9 ppm) into a triazole (**1**–**4**: 4.0–6.6 ppm), leads to a significant downfield shift of the ^{31}P NMR signals, similar to our previous report.[9] Suitable single crystals for X-ray crystallography of compounds **1** and **3** were obtained from slow evaporation of their concentrated solutions in acetone or methanol at room temperature, respectively (Figure 2). The bond lengths and angles (Supporting Information) are in good agreement with previously reported *P*-phenyl dithienophosphole oxides.[4] The unit cell of compound **1** exhibits two independent molecules.

Scheme 1. Synthesis of *P*-Triazole Dithieno[3,2-*b*:2′,3′-*d*]phospholes via Azide–Alkynyl Click Reaction

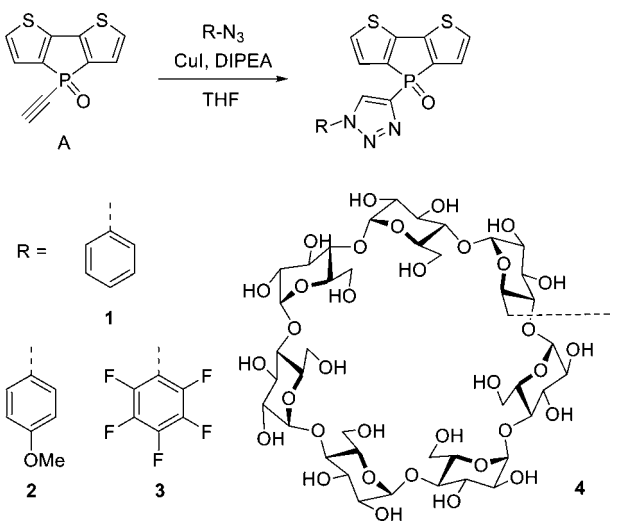

Notably, intermolecular P═O---H–C (triazole) hydrogen bonding (HB) interactions at distances of 3.2 and 3.0 Å (between O and C) for **1** and **3**, respectively, clearly illustrate the noninnocent nature of the triazole unit. The shorter distance in **3** indicates stronger HB interaction, as a result of the electron-withdrawing features of the C_6F_5 moiety. The torsion angles of **1** (36.1° and 21.5°) between the triazole and the P-substituent are smaller that that of **3** (56.6°), partly because of an additional, weaker HB interaction between P═O and H–C (*P*-phenyl). Weak π–π stacking between two neighboring planar dithienophosphole scaffolds is observed for both compounds (d = 3.54 Å for **1**, 3.82 Å for **3**).

Interestingly, in the packing of **3**, six pentafluorobenzene rings form the perimeter of a nanoporous tube with a diameter of ~8 nm, which is partially (ca. 15–20%) occupied by disordered methanol molecules (Figure 2b). The pore volume corresponds to ~12% of the total volume. The effect of the fluorinated benzene ring thus suggests some potential for the engineering of self-assembled materials using these species as building blocks in the context of gas capture and storage.[11]

The photophysical data of the new phosphole compounds are summarized in Table 1. The compounds are highly fluorescent in solution; in CH_2Cl_2, compounds **1**–**3** show very similar absorption (λ_{abs} = 365–367 nm) and emission (λ_{em} = 453–456 nm) features, with comparable quantum yields of about ϕ_{PL} = 0.6. The different lateral aromatic substituents do not exhibit an obvious effect on the photophysical properties, suggesting the unlikeliness of charge-transfer processes from the lateral moiety to the dithienophosphole, which was observed for the triphenylamine system **III** (Figure 1).[8a] This can be attributed to the poor electronic communication between the two units, as

(8) (a) Chua, C. J.; Ren, Y.; Baumgartner, T. *Org. Lett.* **2012**, *14*, 1588–1591. (b) Chua, C. J.; Ren, Y.; Baumgartner, T. *Organometallics* **2012**, *31*, 2425–2436.

(9) He, X. M.; Lin, J. B.; Kan, W. H.; Dong, P.; Trudel, S.; Baumgartner, T. *Adv. Funct. Mater.* **2013**, DOI: 10.1002/adfm.201302294.

(10) (a) Zhang, Y. M.; Han, M.; Chen, H. Z.; Zhang, Y.; Liu, Y. *Org. Lett.* **2013**, *15*, 124–127. (b) Ogoshi, T.; Harada, A. *Sensor* **2008**, *8*, 4961–4982.

(11) (a) Hird, M. *Chem. Soc. Rev.* **2007**, *36*, 2070–2095. (b) Holst, J. R.; Trewin, A.; Cooper, A. I. *Nat. Chem.* **2010**, *2*, 915–920. (c) Mastalerz, M. *Chem.—Eur. J.* **2012**, *18*, 10082–10091.

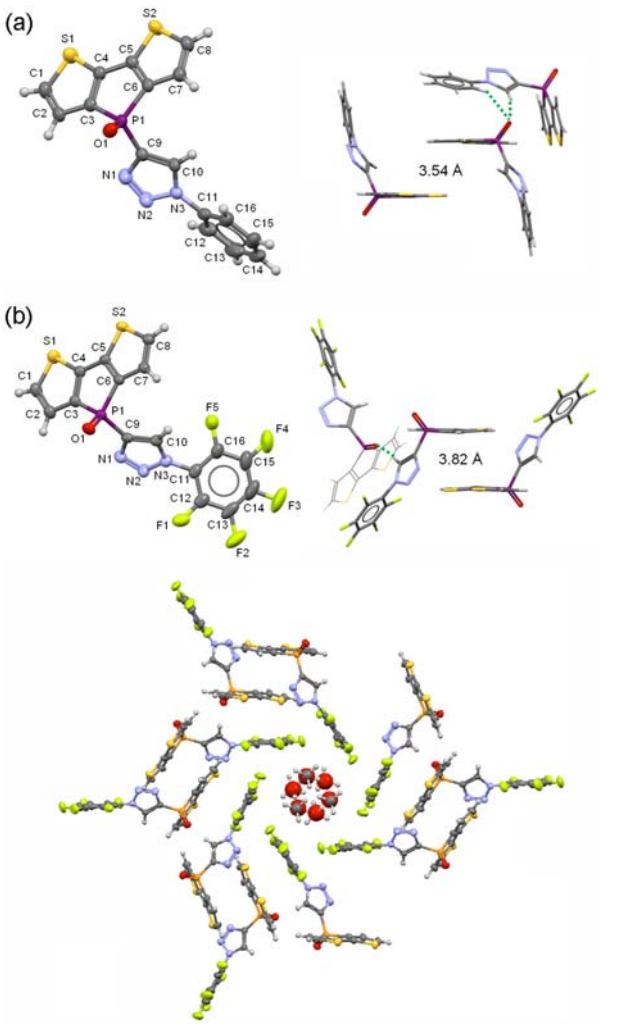

Figure 2. Molecular structures, intermolecular interaction, and supramolecular organization of **1** (a) and **3** (b) in the solid state (50% probability level). Selected bond lengths and angles are shown in Figures S1 and S2, Supporting Information.

confirmed by DFT calculations (vide infra). A modest solvatochromic effect is observed for **1**–**3** in solvents with different polarity (hexanes, CH_2Cl_2, CH_3CN, DMF, CH_3OH), as shown in Figure 3. The Lippert–Mataga plot for **1**–**3** is shown in Figure S3, Supporting Information.[12] In protic solvents, i.e., MeOH, a red shift of $\Delta\lambda_{em} \sim 12$ nm is observed for the emission and tentatively assigned to the stabilization of the excited state by HB between the solvent and the triazole moiety.[13]

Cyclodextrins (CDs) are promising macrocyclic hosts due to their unique hydrophobic cavity allowing for efficient extraction and binding of organic molecules in water.[10] It is well-known that the attachment of fluorophores to the CD scaffold is not only capable of improving the water solubility of the former, but they can also act as fluorescent sensors for organic guest molecules.[10] In this context, we have targeted the new CD-functionalized dithienophosphole **4**. Hybridization with β-CD significantly improves the water solubility of **4** but at the same time maintains its pronounced luminescence. A slight decrease in the quantum yield of **4** (ϕ_{PL} = 0.45) is attributed to the nonrigid CD moiety that opens up nonradiative relaxation pathways.[13] Because of the short CH_2 linker between CD and the dithienophosphole, the luminophore cannot enter the hydrophobic cavity of CD. This is confirmed by the red shift in both the absorption ($\Delta\lambda_{abs}$ = 6 nm) and emission ($\Delta\lambda_{em}$ = 20 nm) of **4** in H_2O, compared to that of **1** in CH_2Cl_2, and which is consistent with the solvatochromism of **1**–**3**. The fixated location of the dithienophosphole should thus allow easy access to the CD cavity for guest molecules without competing with the attached luminophore.[10]

The detection of explosives is a major security concern and development of effective sensory materials to this end is consequently highly valuable.[14] To test the utility of **4** as effective sensory material for explosives, we have selected picric acid as target analyte for our study. As shown in Figure 4, addition of picric acid to an aqueous solution of **4** produced significant fluorescence quenching, with the intensity ratio (I_F/I_0) of 0.39, 0.16, 0.07, and 0.04 in the presence of 1, 2, 3, and 4 equiv of picric acid, respectively, allowing for an easy detection, even with the naked eye. The emission quenching is attributed to an energy and/or electron transfer from **4** to the picric acid acceptor, triggered by the inclusion of the picric acid inside the CD cavity (Figure S5, Supporting Information). A comparable feature has also been observed in other luminescent explosives sensors.[14] Notably, however, this is the first example of a phosphole-based sensor for detection of nitroaromatics in aqueous medium.[15] The binding constant ($\log K_s = 4.80 \pm 0.02$) was obtained from a nonlinear least-squares fit for 1:1 binding (Figure S6, Supporting Information).[16] This value is comparable to the previously reported phosphole oxide sensor system by Shiraishi el al.[15] Importantly, the detection limit for picric acid lies in the nanomolar range and the response time is very fast (seconds). Moreover, the extent of emission quenching of **4** in the presence of 1 equiv of picric acid after 30 s is practically identical to that after 2 h (Figure S7, Supporting Information), confirming the persistence of the inclusion complex.

To obtain a better understanding of the photophysical and electronic properties, density functional theory (DFT)

(12) Filarowski, A.; Kluba, M.; Cieślik-Boczula, K.; Koll, A.; Kochel, A.; Pandey, L.; De Borggraeve, W. M.; der Auweraer, M. V.; Catalán, J.; Boens, M. *Photochem. Photobiol. Sci.* **2010**, *9*, 96–1008.

(13) (a) Lakowicz, J. R. *Principles of Fluorescence Spectroscopy*, 3rd ed.; Springer: New York, 2006. (b) Valeur, B. *Molecular Fluorescence, Principles and Applications*; Wiley-VCH: Weinheim, 2002.

(14) (a) Yang, J.-S.; Swager, T. M. *J. Am. Chem. Soc.* **1998**, *120*, 5321–5322. (b) Sohn, H.; Sailor, M. J.; Magde, D.; Trogler, W. C. *J. Am. Chem. Soc.* **2003**, *125*, 3821–3830. (c) Kartha, K. K.; Babu, S. S.; Srinivasan, S.; Ajayaghosh, A. *J. Am. Chem. Soc.* **2012**, *134*, 4834–4841. (d) Novotney, J. L.; Dichtel, W. R. *ACS Macro Lett.* **2013**, *2*, 423–426.

(15) Shiraishi, K.; Sanji, T.; Tanaka, M. *ACS Appl. Mater. Interfaces* **2009**, *1*, 1379–1382.

(16) He, X. M.; Lam, W. H.; Zhu, N.; Yam, V. W. W. *Chem.—Eur. J.* **2009**, *15*, 8842–8851.

Table 1. Photophysical and DFT Data for **1**–**4**

				TD-DFT[c]			DFT[c]		
compd	λ_{abs}/nm[a] (ε/dm^3 mol^{-1} cm^{-1})	λ_{em}[a]/nm	Φ_{PL}[b]	λ/nm	f	transition[d]	LUMO	HOMO	E_g
1	365 (5431)	453	0.61	372	0.1857	H→L (83%)	−1.91	−5.82	3.91
2	365 (5878)	453	0.63	371	0.1871	H→L (83%)	−1.84	−5.76	3.92
3	367 (6162)	456	0.62	374	0.1751	H→L (84%)	−2.04	−5.93	3.89
4	371 (6446)	473	0.45						

[a] In CH_2Cl_2 solution at 298 K. [b] Fluorescence quantum yield, relative to quinine sulfate (0.1 M H_2SO_4 solution); excitation at 365 nm. [c] Calculated with Gaussian 09, revision A.02; B3LYP/6-31G(d) level of theory. [d] λ = wavelength, f = oscillator strength, H = HOMO, L = LUMO; coefficient percentage of orbitals involved in the transition.

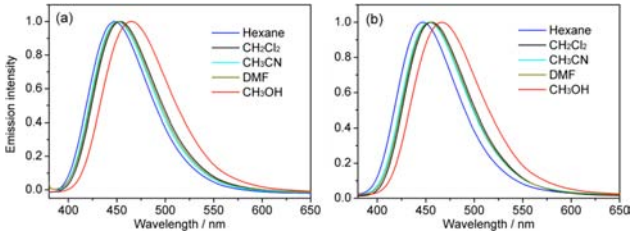

Figure 3. Normalized emission spectra for the solvatochromic studies of **1**(a) and **3** (b).

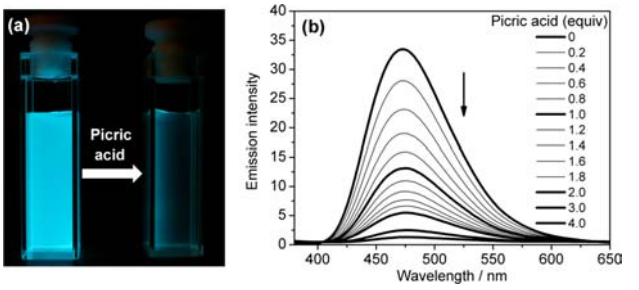

Figure 4. Changes in the emission color(a) and emission spectra (b) of **4** (5.0×10^{-5} M) in water upon addition of picric acid, excitation at 365 nm.

calculations (B3LYP/6-31G(d)) were performed.[17] The HOMO and LUMO orbital diagrams and energy levels of **1**–**3** are shown in Figure S8 (Supporting Information) and Table 1. The HOMO orbitals represent the π-systems of the conjugated backbone and the lone pair on the oxygen atom. The LUMO orbitals mainly consist of the π^*-systems of the conjugated backbone and some minor contribution from the triazole moiety. Almost no contribution from the aromatic groups connected to triazole unit is observed, suggesting the absence of any potential charge-transfer processes. As expected, increasing the electron-acceptor properties of the lateral aromatic groups leads to a stabilization of both the HOMO and LUMO energies. However, the calculated energy gaps (E_g), **1** (3.91 eV) = **2** (3.91 eV) > **3** (3.89 eV), are fully consistent with the observed photophysics (λ_{em}: **1** = **2** < **3**). Furthermore, the calculated UV/vis spectra from time-dependent DFT (TD-DFT) also agree very well with the experimental data. The UV/vis absorptions mainly come from π–π^* HOMO −LUMO transitions, with significant contributions of 83–84%.

In summary, we have reported the synthesis of functional dithienophospholes and a cyclodextrin-based sensor for detection of nitroaromatic-based explosives in water. Due to poor electronic communication, the effect of the lateral aromatics on the photophysical properties of the main scaffold is negligible. However, the slight change from phenyl to pentafluorophenyl as lateral aromatic group leads to significantly different molecular packing in the solid state, highlighting the promising potential of this new class of compounds for the crystal engineering of functional solid-state materials.

Acknowledgment. Financial support by the NSERC of Canada, as well as the Canada Foundation for Innovation (CFI), is gratefully acknowledged. S.E.N.M. thanks MITACS Globalink for a scholarship.

Supporting Information Available. Experimental procedures and characterization data for **1**–**4**, X-ray crystal data, structure refinement and selected bonds and angles for **1** and **3**, optimized structure coordinates of **1**–**3** (DFT), and complete ref 17. This information is available free of charge via the Internet at http://pubs.acs.org.

(17) Frisch, M. J.; et al. *Gaussian 09*, revision A.02; Gaussian, Inc.: Wallingford, CT, 2009. See the Supporting Information for the full reference.

The authors declare no competing financial interest.